CHAPTER 5

Steel Reinforcement Effectiveness to Combat Reflective Cracking in Rehabilitation Applications

5.1 ABSTRACT

While field performance is the only true indicator of whether steel reinforcement is effective in delaying the reflection of cracks, analytical techniques may help to predict field performance, thus allowing for better planning and utilization of available funds. In this chapter, 3D finite element (FE) techniques are used to validate the effectiveness of steel reinforcement in delaying the reflection of cracks. This analysis considered both the crack initiation and propagation phases. The crack initiation is described using a traditional fatigue law developed by the Belgium Road Research Center (BRRC), and the crack propagation phase is described using Paris-Erdogan phenomenological law. The results presented in this chapter demonstrate that steel reinforcement is effective in delaying the reflection of cracks by positively contributing to the crack initiation and propagation phases. The percentage of improvement to the crack initiation phase ranged between 10 and 40%, depending mainly on the overlay thickness. Thicker overlays more effectively enhanced this improvement. In the crack propagation phase, the percentage improvement ranged between 40 and 170%, depending on the stiffness of the surrounding layers and their thicknesses. Steel reinforcing nettings greatly improved the performance of the 50-mm overlay; the interlayer system mainly influenced the pavement behavior at a shallow depth from its location. Overall, steel reinforcement improves the pavement total service life against reflective cracking by a factor ranging between 50 and 90%.

5.2 INTRODUCTION

Different methods, including the use of interlayer systems, have been suggested for enhancing pavement resistance to reflective cracking. Experimental investigations in the early 1980s showed that interlayer systems might be used to delay or to prevent the reflection of cracks through a new overlay laid over an old cracked pavement (Halim et al. 1983; Kennepohl et al. 1985). Later, Button and Lytton (1987) postulated that the use of interlayer systems to mitigate reflective cracking can be achieved by using two different mechanisms: reinforcement of HMA with a stiff interlayer to provide a better distribution of the applied load over a larger area and to compensate for the lack of tensile strength of the HMA; and dissipation of strain energy in the vicinity of the cracked through the use of a soft layer. It is important to realize that a material would provide reinforcement to the surrounding medium only if it is stiffer than the material that needs to be reinforced (Rigo 1993). Within the contest of this study, a reinforcing material would have to be stiffer than the HMA material.

In Chapter 3, analytical modeling was used to explain how a specially designed geocomposite membrane may be used to delay the reflection of cracks in flexible pavements by acting as a strain energy absorber. It was shown that the soft interlayer was able to dissipate energy around the cracked region**;** however, this increases the pavement flexibility.

In this chapter, an analytical approach is used to demonstrate the ability of steel reinforcing nettings to delay reflective cracking. The mechanism by which steel reinforcing nettings can improve pavement resistance to reflective cracking is explained in the following chapter and used to develop design equations. The necessary background related to the reflective cracking failure mechanism is presented in Chapter 3 and is extended in this chapter to the three-dimensional case. The following section summarizes some recent investigations regarding the effectiveness of steel reinforcing nettings in combating reflective cracking (a complete review of the existing literature related to this subject is presented in Appendix A).

5.3 BACKGROUND

Based on field and theoretical investigations, the new class of steel reinforcement has been evaluated in several applications (Brown et al. 2001; Coni and Bianco 2000; Francken and Vanelstraete 1992); some are described in this section. In 2000**,** Vanelstraete and Francken presented Belgium's experience with steel reinforcement (Vanelstraete and Francken 2000). Six different sites incorporating steel reinforcement (and polyester non-woven geotextile), built between 1989 and 1995, were evaluated for their effectiveness in preventing reflective cracking. All sites used HMA overlays on existing jointed concrete pavements. Based on field evaluation, Vanelstraete and Francken found that steel reinforcement is effective in reducing the reflection of cracks. In general, the performance of the overlay was enhanced if slab-fracturing techniques were used prior to placement of the overlay, as these techniques reduced vertical movements at the joints. However, this procedure also reduced the overall bearing capacity of the existing pavement, which had to be balanced by a slight increase in the overlay thickness. Vanelstraete and Francken also concluded that overlay thickness still remains the major factor in overlay performance.

A project in Mont-Saint-Aubert, Belgium was among the six test sites that Vanelstraete and Francken evaluated. The pavement was a highly deteriorated rigid pavement system with a traffic pattern classified as light to medium (see Figure 5-1a). In 1989, steel-reinforcing netting was installed after minor repairs were made to the existing pavement structure. A 70mm overlay was then applied on top of the steel mesh. After 10 years of service, inspections of this site showed a reflective crack occurrence of only 1% (Vanelstraete and Francken 2000). Figure 5-1b illustrates the same road in 2000 after 11 years of service (after Al-Qadi et al. 2002). Other sites also demonstrated notable reductions in reflective cracking when steel reinforcement was used.

Makela et al. presented the Finnish experience with steel reinforcement**,** based on the evaluation of ten different sites in which steel reinforcement was used to enhance the bearing capacity of the road and prevent pavement damage by frost heave (Makela et al. 1999). It is worth noting that steel reinforcement was sometimes installed at two different locations within the same pavement structure (inside the base layer, and on top

of the existing pavement prior to the overlay installation). This test site has functioned well for over twelve years without major problems. It should also be noted that the steel mesh product used was not hexagonal in shape, but rectangular. Furthermore, the reinforcement was not placed in the transversal direction, but in the longitudinal direction (parallel to the direction of traffic). The authors reported that, in all the test sites, steel reinforcement prevented frost damage, which usually appears as longitudinal cracks in the pavement surface, while the control sections showed significant damage.

(a) (b)

Figure 5-1. Comparison between a Road in Belgium: before Repair and 11 years after Repair (after Al-Qadi et al. 2002)

Brown et al. investigated the effectiveness of different interlayer systems (geogrid, steel reinforcement, and glass fiber) in preventing the reflection of cracks in HMA overlays (Brown et al. 2001). A repeated load shear test was first used to evaluate the interface shear strength and stiffness for unreinforced and reinforced samples. A semi-continuous fatigue test fixture was then utilized to evaluate the fatigue life of a 400 x 200 x 90mm-thick beam sample. Reinforcement was placed 30mm above the base, and support was provided by two rubber layers placed over a steel base. A laboratory testing set was performed concurrently to evaluate the effect of interlayer systems on thermally induced loading due to the expansion and contraction of a concrete base. This fixture simulated a HMA overlay over a jointed concrete. The joint was slowly opened until failure of the specimen occurred.

This study indicated that steel reinforcement provides interface shear stiffness comparable to the unreinforced case. Brown et al. (2001) suggested that steel reinforcement might improve the fatigue life by a factor of up to three times. They also found that steel reinforcement is effective in preventing reflective cracking due to the thermal movement of a concrete slab.

5.4 STEEL REINFORCEMENT EFFECTIVENESS

While field performance is the only true indicator of whether steel reinforcement is effective in delaying the reflection of cracks, analytical techniques may help to predict field performance. This allows for better planning and more efficient utilization of available funds. However, the calibration and adjustment of any theoretical model is necessary to ensure the accuracy of the developed models to simulate pavement performance. The following sections present the predicted performance against reflective cracking failure utilizing a FE approach for steel-reinforced and regular overlay rehabilitation strategies.

5.4.1 Background

Consider a cracked isotropic elastic infinite plate subjected to a biaxial state of stress, resulting in a Mode I loading (see Figure 5-2); it can be shown that the stress field in the vicinity of the crack tip may be described using the following relations (Broek 1982; similar equations may be derived for Mode II and Mode III loading):

$$\sigma_x(r,\theta) = \frac{K_I}{\sqrt{2\pi r}}\cos\frac{\theta}{2}\left(1-\sin\frac{\theta}{2}\sin\frac{3}{2}\theta\right) \tag{5.1}$$

$$\sigma_y(r,\theta) = \frac{K_I}{\sqrt{2\pi r}}\cos\frac{\theta}{2}\left(1+\sin\frac{\theta}{2}\sin\frac{3}{2}\theta\right) \tag{5.2}$$

$$\tau_{xy}(r,\theta) = \frac{K_I}{\sqrt{2\pi r}}\sin\frac{\theta}{2}\cos\frac{\theta}{2}\cos\frac{3}{2}\theta \tag{5.3}$$

where

r and θ = polar coordinates originating at the crack tip; and

K_I = stress intensity factor associated with Mode I loading.

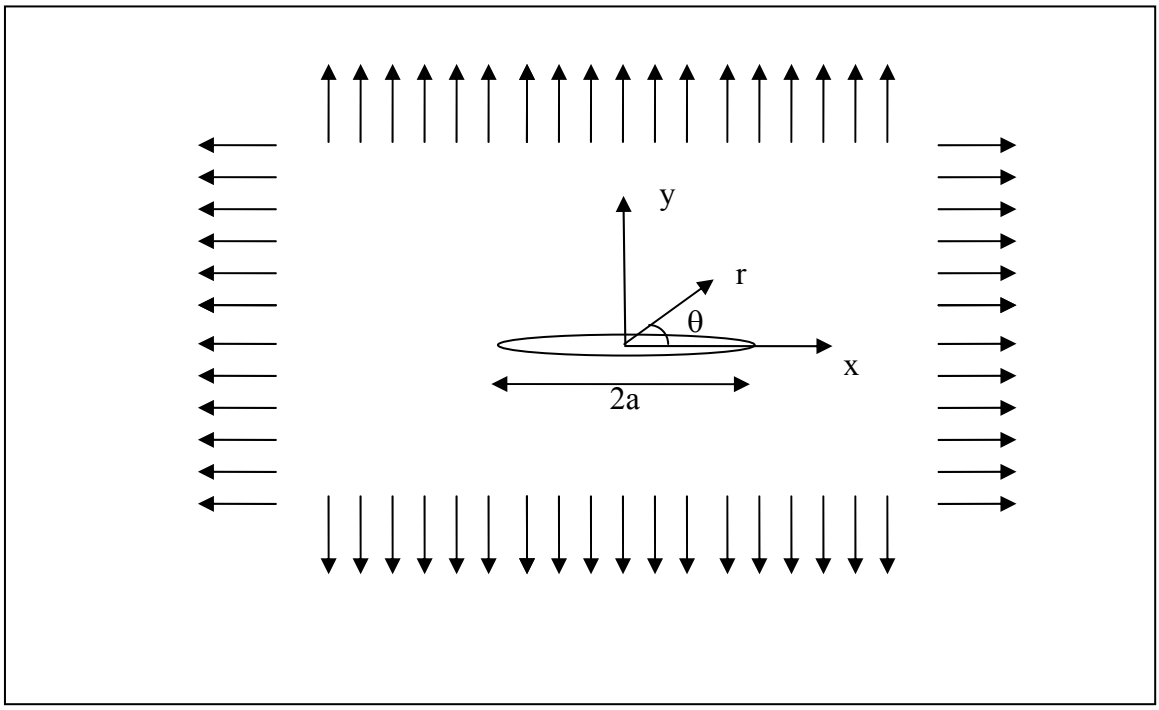

Figure 5-2. Mode I Crack Under Bi-Axial State of Stresses

It may be noticed from these equations that the main characteristic of the stress field in the vicinity of the crack is that all the stresses go to infinity at the crack tip ($r \rightarrow 0$). This is known as the singularity of the stress field at the crack tip. This is a characteristic of the elastic solution, which neglects the occurrence of plastic deformations around the crack tip. As equations (5.1) to (5.3) demonstrate, the order of the singularity for elastic problems is $r^{-0.5}$. For perfect plasticity, the order of the singularity is r^{-1}. Different orders of singularity may be defined depending on the considered constitutive behavior.

To simulate a singularity of order $r^{0.5}$ using ABAQUS finite element solver, the mid-side nodes of 20-node brick elements (C3D20R) along the sides of the cracks are moved to the quarter positions next to the crack tip. To validate the singularity, all

elements around the crack tip start as cubic elements, and then are "collapsed" to form pyramidal elements (see Figure 5-3).

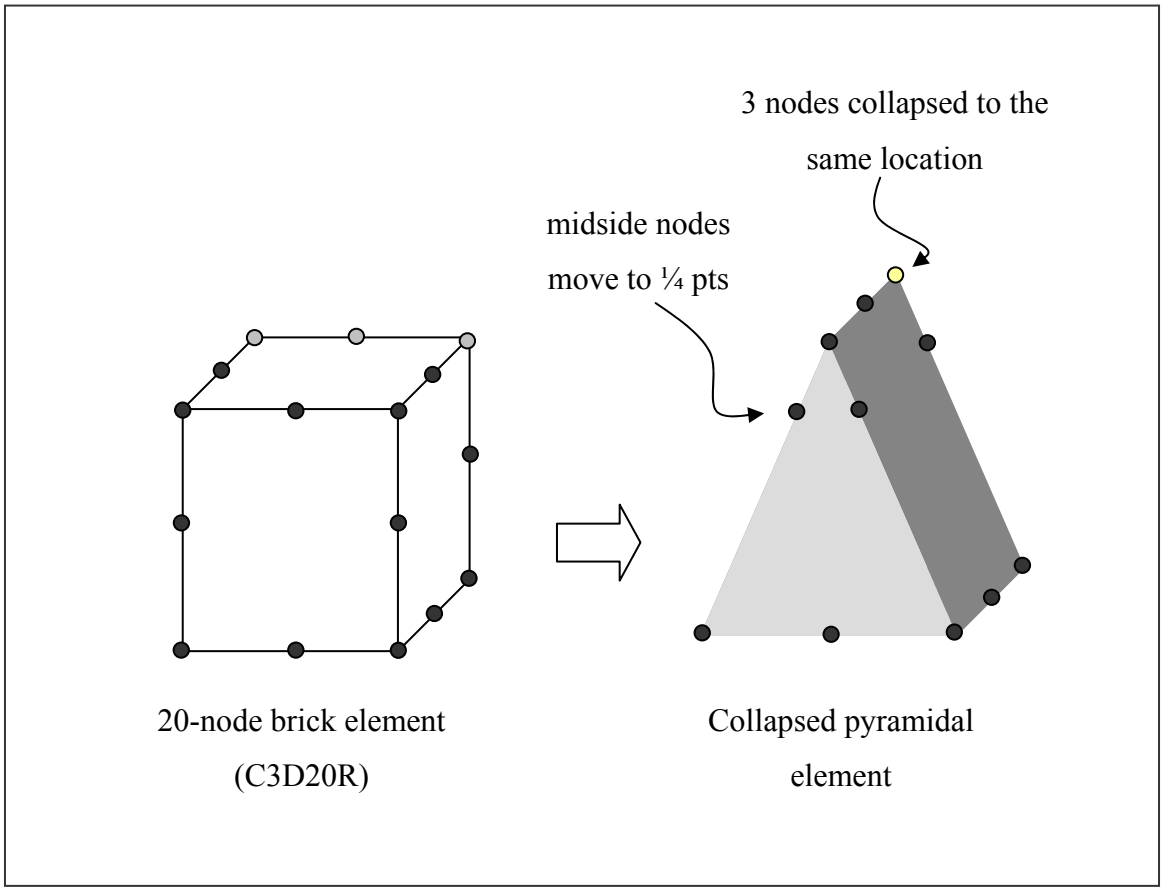

Figure 5-3. Collapsed Three-Dimensional Brick Element

The stress intensity factor is usually considered a measure of the whole stress field at the crack tip. Crack propagation will occur when the stress intensity factor reaches a critical value K_{Ic}, known as the fracture toughness of the material. In contrast to the stress intensity factor, the fracture toughness is a quantity that is independent of the crack geometry.

It was previously indicated that no exact definition of the stress intensity factor for a multi-layer pavement system is available (see Chapter 3). An effective method to characterize and calculate the stress intensity factor for the problem at hand is by using

the path independent integral, called the J-integral. The J-integral is defined as the change in mechanical energy per unit area of new crack surface (Rice 1968):

$$J = \int_{\Gamma} \left(U dn - T \frac{\partial u}{\partial x} ds \right) \tag{5.4}$$

where

Γ = a curve that surrounds the crack tip;

U = strain energy density;

n = direction normal to the crack line;

T = traction vector;

u = displacement vector; and

ds = differential element of arc Γ.

In contrast to the complexity associated with the calculation of the stress intensity factor, the J-integral is easily calculated around the crack front by simulating different contour lines around the crack tip. Each contour is a ring of collapsed elements completely surrounding the crack front from one crack face to the opposite face. The number of evaluations possible is dependent upon the number of such rings of elements (ABAQUS 1998). After the calculation of the J-integral, the stress intensity factor may be determined as follows (assuming plane strain condition and considering an equivalent stress intensity factor for the considered loading pattern):

$$J = \frac{1 - \nu^2}{E} (K_{eq}^2) \tag{5.5}$$

where

υ = Poisson's ratio;

E = Elastic modulus; and

K_{eq} = Equivalent stress intensity factor associated with the considered loading pattern.
Since the stress intensity factor is a measure of the stress and strain environment around the crack tip (a greater stress intensity factor indicates a faster rate of propagation), the rate of fatigue crack propagation per cycle (da/dN) depends upon the stress intensity factor amplitude during the cycle (ΔK). A description of the crack propagation phase in flexible pavements can be based on the empirical power law developed by Paris and Erdogan (1969):

$$\frac{dc}{dN} = A(\Delta K)^n \tag{5.6}$$

where
c = crack length;
N = number of loading cycles;
A and n = fracture parameters of the material; and
ΔK = stress intensity factor amplitude.

The use of this empirical equation is generally accepted among pavement researchers to describe the rate of crack growth in HMA overlay**,** assuming continuous crack growth in HMA and given the small size of the developed plastic zone with respect to the problem size (Erkens 1997; Uzan 1997).

5.4.2 Theoretical Investigation

Several FE models were developed to simulate a variety of four-layer systems that are regularly encountered in typical flexible pavement overlay applications (see Table 5-1). In this partial factorial design, seven different factors are considered and are presented in Table 5-1. A total of 432 different pavement designs were analyzed to develop the suggested design equations presented in the following chapter. The simulated pavement structures consist of an existing cracked HMA layer, a base layer, on top of a subgrade.

A HMA overlay with variable thicknesses is applied to the cracked HMA layer. To investigate the crack initiation and propagation phases, three-dimensional (3D) models were developed for different locations of the cracks. A 3D crack was induced in the existing HMA layer (see Figure 5-4). A square root singularity ($r^{1/2}$) was considered for the developed model. This type of singularity is suitable for the linear elastic problem. This focused mesh also enables evaluation of the J-integral through different contour lines at different location along the crack front (three contour lines are shown in Figure 5-4).

The simulated cracking condition represents a crack that propagated through the entire thickness of the existing HMA (full depth crack). A less severe cracking pattern, which represents a surface crack that is only present at the top of the HMA layer, was not considered in this study. In a previous study, Jacobs et al. (1992) showed that a surface crack will reflect much slower through the overlay than will a full depth crack. It should also be noticed that a more accurate simulation of the crack may have been achieved through a better mesh refinement. However, a coarser mesh was selected in order to preserve the continuity of the nodes between the layers and steel reinforcement. This continuity was essential for ensuring that the developed stresses around the loading area would be adequately transferred between the nodes, and that unrealistic movement of the nodes would be avoided. It was previously shown (see Chapter 4) that the jump in stresses at the pavement layer interfaces for the considered element dimensions (6.35mm) was less than 17kPa, which represents approximately 2.5% of the applied load. However, this level of accuracy was not applicable for the base layer (element thickness was 25.4mm), which was modeled using a coarser mesh to reduce the required computation time.

The dimensions and geometries of this model (560mm x 38000mm) were similar to those of the models presented in Chapter 4. Similarly, the movement of the load at a speed of 8km/hr was achieved by gradually shifting the loading area over the refined element path (shown in gray in Figure 5-4). Contact between the overlay and the existing HMA layer was assumed fully bonded. Bonding between the existing HMA and the base layers was assumed to a friction-type contact (coefficient of friction = 1.0).

Table 5-1. Layer Characteristics of Pavement Systems

Overlay Thickness (mm)	Overlay Modulus (MPa)	HMA Thickness (mm)	HMA Modulus (MPa)	Base Thickness (mm)	Base Modulus (MPa)	Subgrade Modulus (MPa)
50	3450 (0.25)	100	1725 (0.30)	150	205 (0.35)	40 (0.40)
100	4480 (0.25)	150	2065 (0.30)	300	410 (0.35)	135 (0.40)
150	5510 (0.25)	200	2415 (0.30)	600		

* Poisson's ratio is presented in parenthesis.

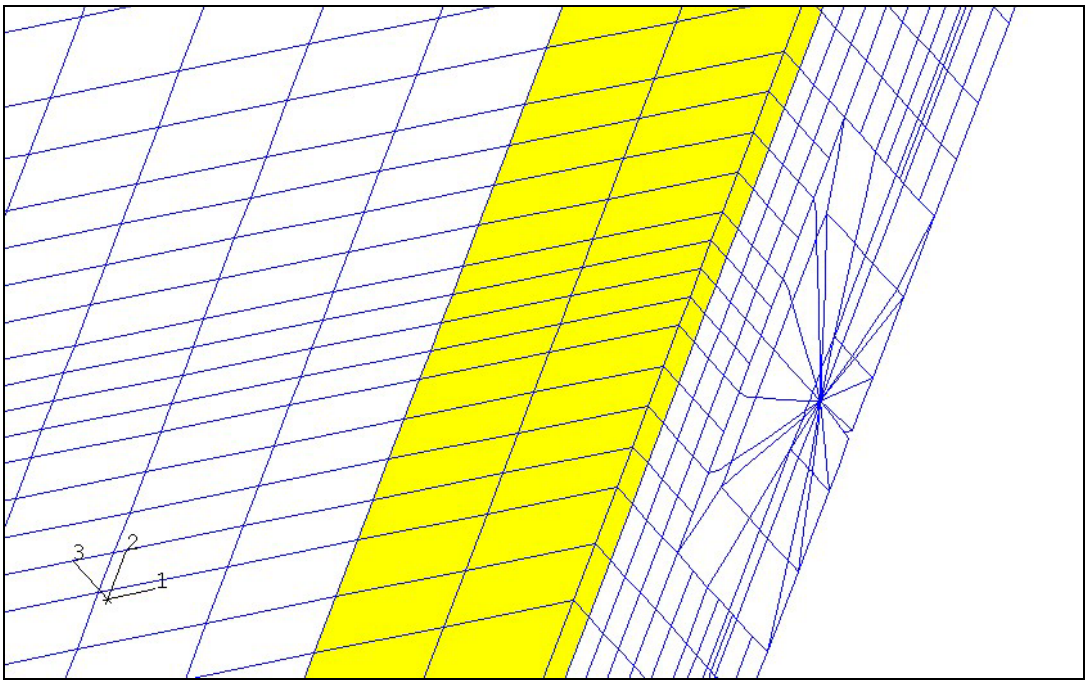

(a)

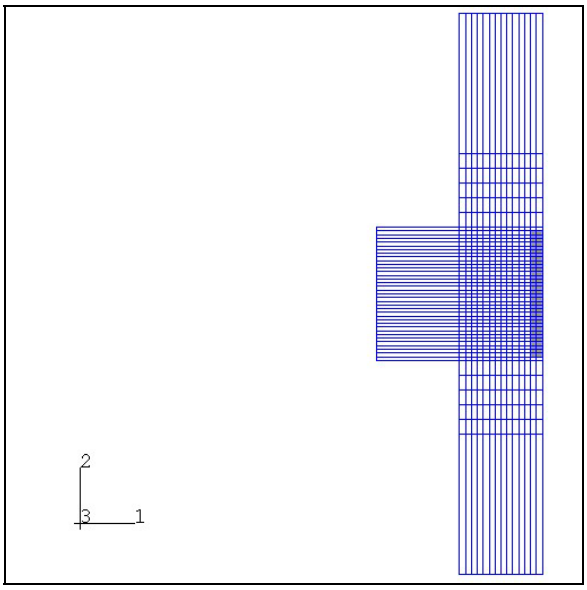

(b)

Figure 5-4. General Layout of the Developed Finite Element Model

5.4.3 Crack Initiation

After placement of the overlay, the existing crack continues to move due to traffic and thermal stresses until it is able to break into the bottom of the overlay. The number of cycles for crack initiation may be determined using the BRCC equation (BRCC 1998):

$$N = 4.856 \times 10^{-14} \varepsilon_{zx}^{-4.76} \tag{5.7}$$

where

N = Number of cycles before crack initiation; and

ε_{zx} = Shear strains 10mm above the existing crack.

The use of this equation requires the calculation of the maximum shear strain 10mm above the crack tip. For each considered pavement structure and at the original position of the crack, the maximum shear strain was calculated. This enabled the calculation of

the number of cycles for crack initiation for all pavement structures considered in this study.

Steel reinforcement was found to significantly reduce the severity of stresses around the crack tip. As shown in Figure 5-5, steel reinforcement clearly reduced the computed J-Integral when the crack tip was underneath the interlayer system. This contribution was independent of the stiffness of the surrounding layers.

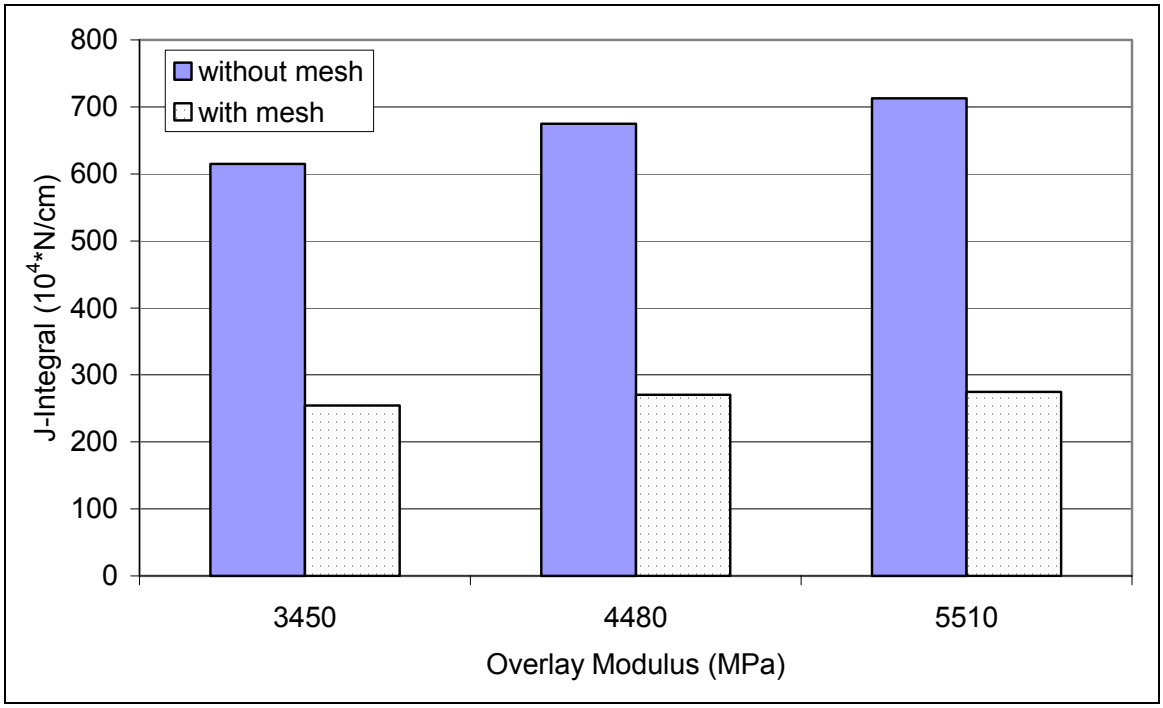

Figure 5-5. J-Integral prior to Crack Propagation in the Overlay ($H_{overlay}$ = 50mm)

Compared to regular overlay structures, reinforced overlays were able to sustain a larger number of cycles before crack initiation. Depending on the overlay thickness (greater enhancement was manifested for thicker overlays), this improvement ranged from 10 to 40%. Figure 5-6 illustrates the percentage increase in the number of cycles for crack initiation with and without steel reinforcement. It can be noticed from this figure that the mesh contribution increases linearly with the overlay thickness. A full coverage of the results of this analysis is presented in Appendix D. The percentage improvement is calculated as follows:

$$I(\%) = \frac{N_r - N_u}{N_u} x100 \quad (5.8)$$

where

N_r = Number of cycles (initiation, propagation, or total) for the reinforced case; and

N_u = Number of cycles for the unreinforced case.

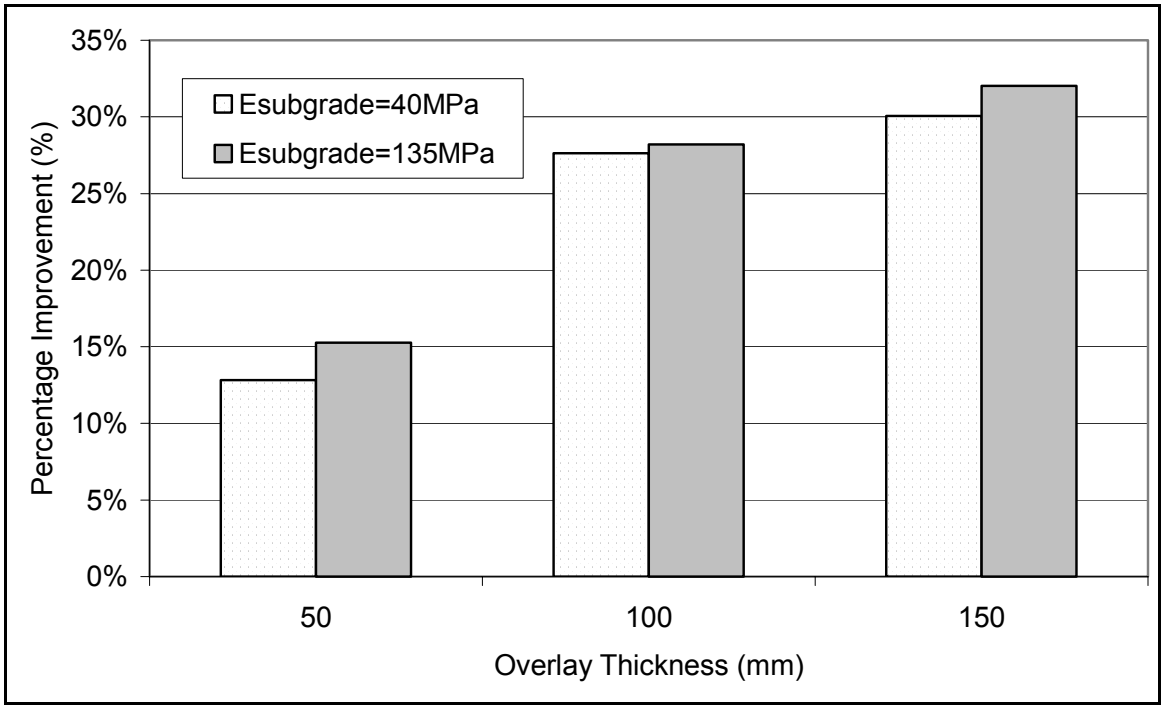

Figure 5-6. Effect of Steel Reinforcement on the Number of Cycles for Crack Initiation

5.4.4 Crack Propagation

As previously indicated, the J-integral was calculated for different locations of the crack in the overlay. The stress intensity factor (K) was then calculated from Equation (5.5). Figure 5-7 illustrates the variation of the stress intensity factor (calculated from the J-integral) for a 100mm overlay thickness for different overlay moduli. As presented in

this figure, the stress intensity factor gradually increased until it reached its maximum at the surface.

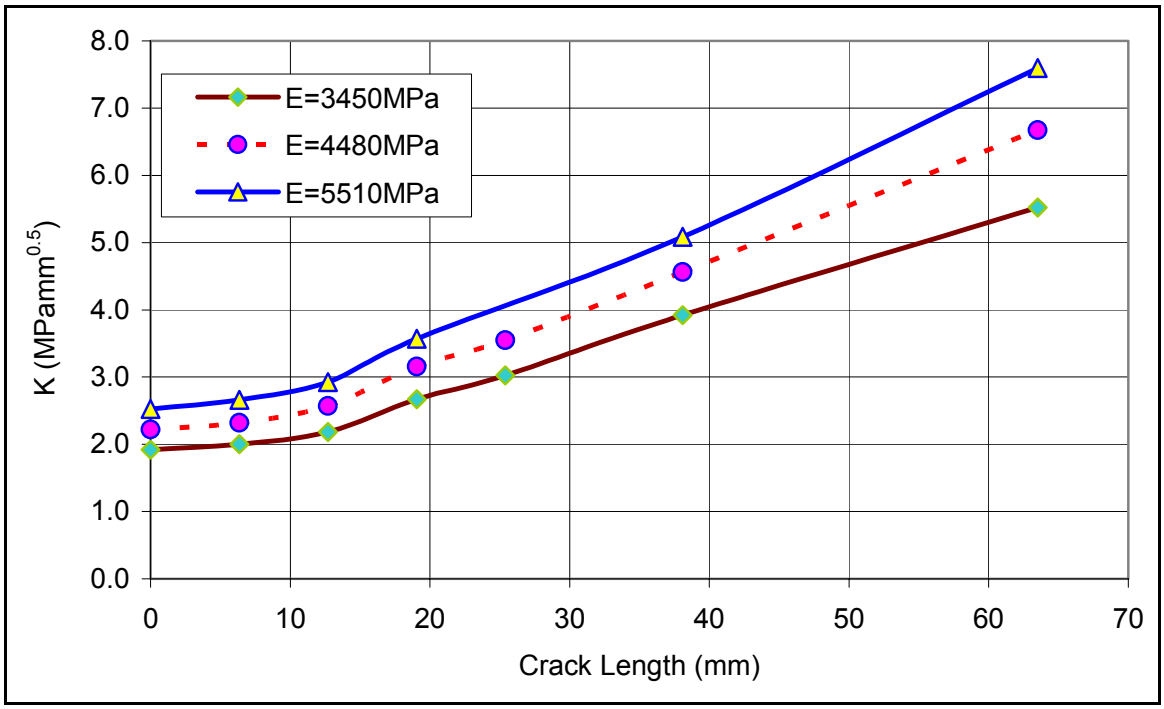

Figure 5-7. Variation of the Stress Intensity Factor with the Crack Length

The stress intensity factor increased with the increase of the overlay modulus. The same trend was previously reported by Uzan (1997). This may explain the superior performance of stone matrix asphalt (SMA), although its resilient modulus is always reported lower than that of conventional mixes (Brown 1992). However, the fracture parameters (A and n) also vary with the material stiffness and crack resistance. Therefore, the HMA resilience modulus may not be used solely to indicate the pavement fracture performance.

Equation (5.6) was used to evaluate the number of cycles for crack propagation. To characterize the variation of the stress intensity factor with the crack length, polynomial regression models were fitted for each investigated case, as shown in Figure 5-8. Although the degree of the polynomial was sometimes reduced from a second degree to a first degree polynomial to avoid convergence difficulties within the

integration, the coefficient of determination (R^2) was always greater than 0.90. To improve the level of convergence, numerical integration was used using Mathematica version 4-2.

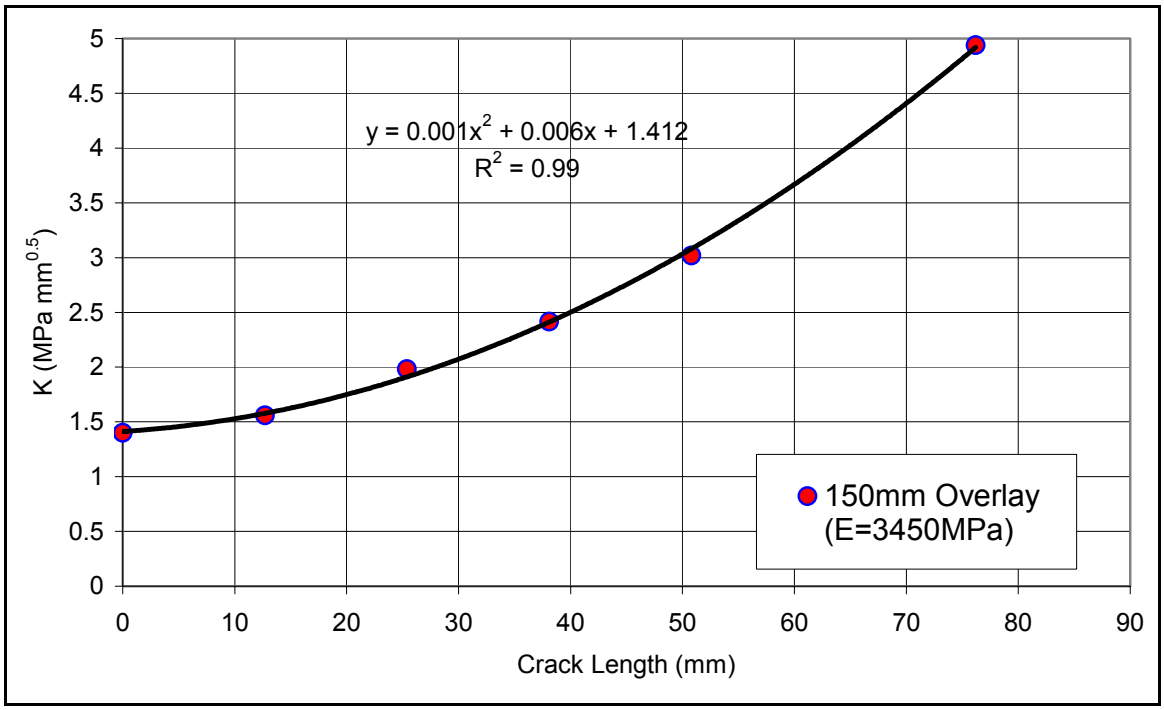

Figure 5-8. Variation of Stress Intensity Factor with Crack Length

Steel reinforcement was found to significantly reduce the stress intensity factor (see Figure 5-9), especially when the crack propagated at a shallow depth from the interlayer's location. This contribution was pronounced for all pavement structures simulated in this study. Results of this analysis are presented in Appendix D and are further discussed in the following chapter.

Figure 5-10 shows the average percentage increase in the number of cycles for the crack to propagate to 12.7mm from the overlay surface due to steel reinforcement. In general, the percentage improvement ranged from 40 to 170%**,** depending on the stiffness of the overlay and the existing pavement structure. Although significant improvement is introduced by steel reinforcement, the overlay thickness remains a major factor in the pavement performance against reflective cracking.

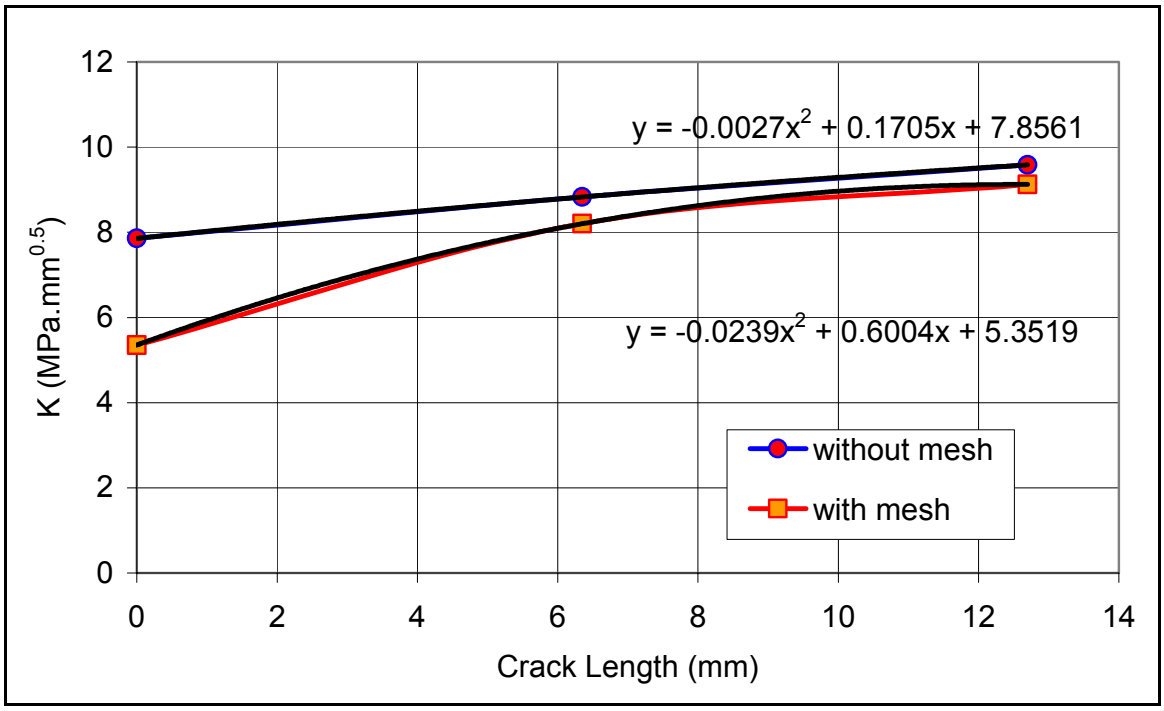

Figure 5-9. Variation of the Stress Intensity Factor with and without Steel Reinforcement for a 50mm Overlay

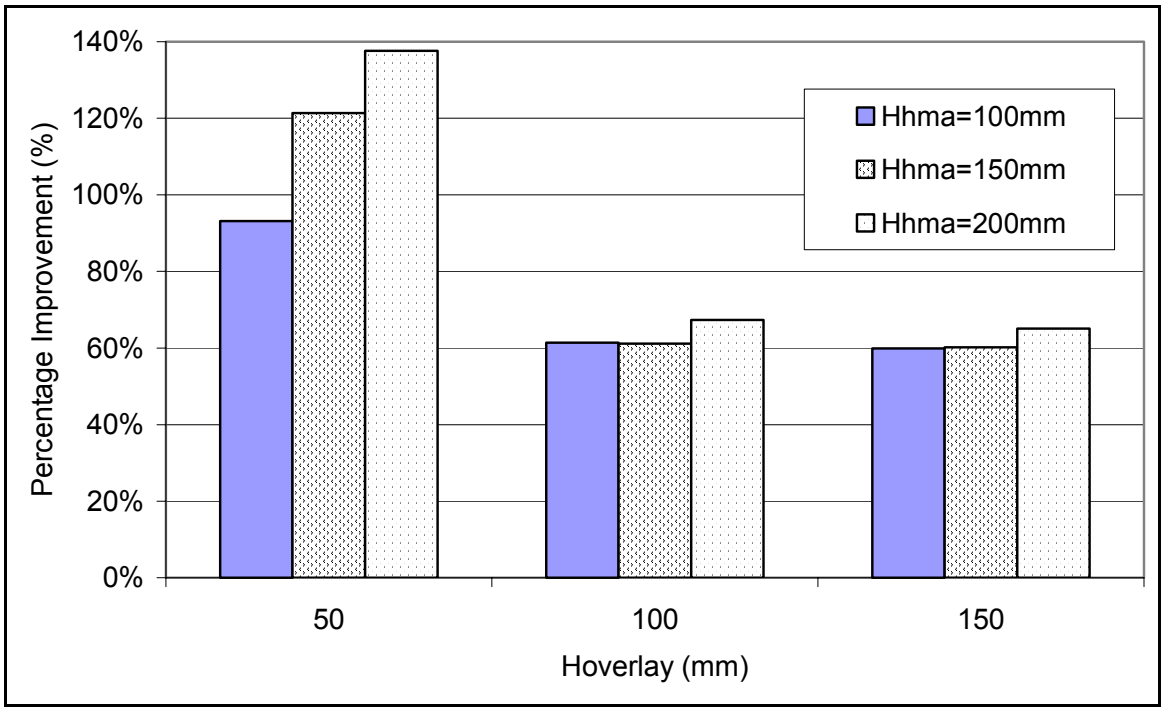

Figure 5-10. Effect of Steel Reinforcement on the Number of Cycles for Crack Propagation

Figure 5-10 demonstrates that the mesh contribution is more pronounced for an overlay thickness of 50mm. The steel reinforcement contribution is most significant as the crack propagates at a shallow depth from the interlayer. As shown in Figure 5-11, steel reinforcement's contribution to the stress intensity factor becomes negligible after the crack propagates to a depth greater than 25.4mm from the interlayer. This indicates that the mesh contribution to the propagation phase is not really dependent on the overlay thickness, in contrast to the crack initiation phase. The closer the crack is to the interlayer, the more pronounced the steel reinforcement contribution.

Based on the results of the investigated cases, Figure 5-12 shows the percentage contribution of steel reinforcement to the calculated total number of cycles until the crack reaches 12.7mm from the overlay surface. This represents the summation of the number of cycles for both crack initiation and propagation. In general, the percentage improvement due to steel reinforcement ranged between 50 and 90%, depending on the overlay thickness and the existing conditions of the pavement structure.

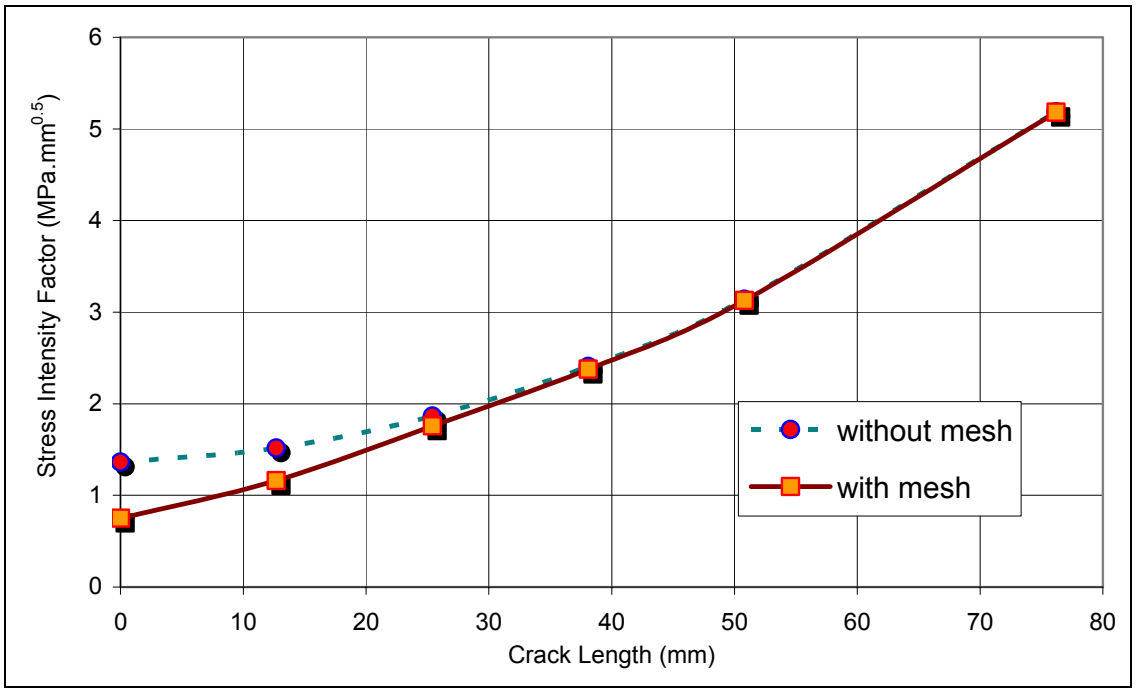

Figure 5-11. Variation of the Stress Intensity Factor for a 150mm Overlay

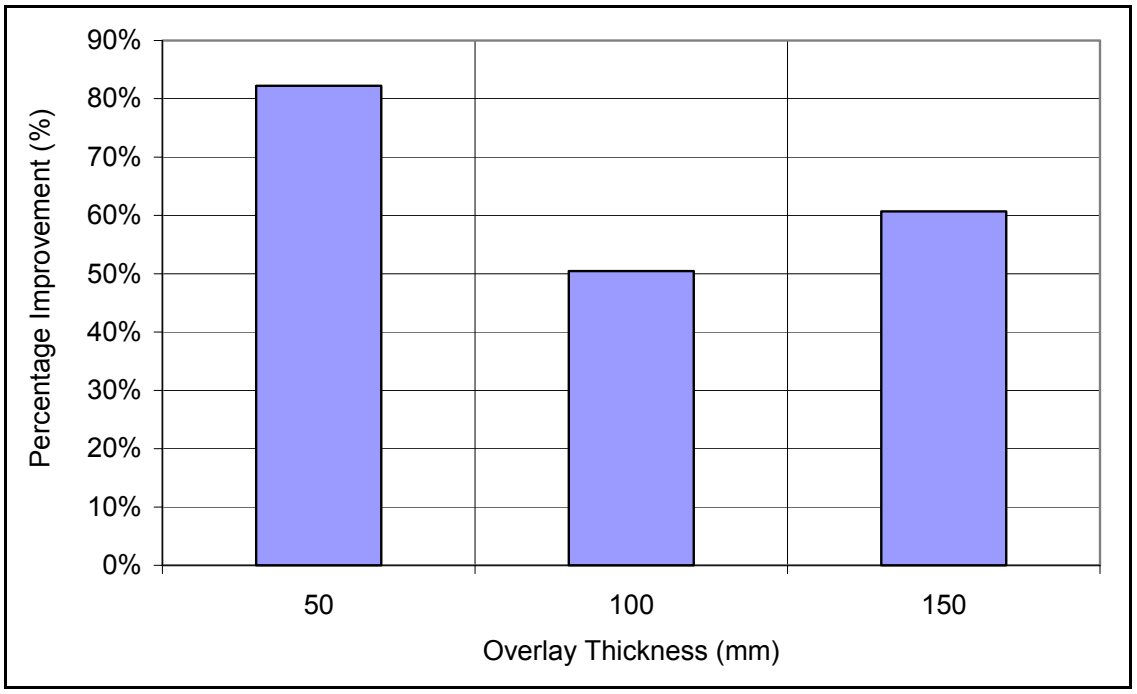

Figure 5-12. Steel Reinforcement Contribution to the Total Service Lives against Reflective Cracking

5.5 FINDINGS AND CONCLUSIONS

A simplified approach was presented to calculate the number of cycles a pavement can endure before an existing crack is able to initiate and propagate to the new overlay surface. This approach, which is based on a 3D FE technique and fracture mechanics principles, can be used to derive simple regression models that can predict pavement service life against reflective cracking. Based on the results presented in this chapter, the following conclusions may be drawn:

- Steel reinforcement is effective in delaying the reflection of cracks during the crack initiation and propagation phases.
- The percentage improvement to the crack initiation phase ranged between 10 and 40%, mainly depending on the overlay thickness. Thick overlays manifested greater enhancement.

- The percentage improvement to the crack propagation phase ranged between 40 and 170%, depending on the stiffness of the surrounding layers and their thicknesses. A greater contribution is expected for the 50-mm overlay; the closer the crack is to the reinforcing interlayer, the greater its effectiveness to delay reflection cracks.
- The percentage improvement to the total pavement service life against reflective cracking ranged between 50 and 90%, depending on the overlay thickness and the condition of the existing pavement system.

5.6 REFERENCES

"ABAQUS, Finite Element Computer Program." (1998). Version 5.8, Hibbitt, Karlsson and Sorensen, Inc, MI.

Al-Qadi, I. L., Elseifi, M. A., and Freeman, T. E. (2002). "Steel reinforcing netting mechanism to abate reflective cracking in asphalt concrete overlays." Paper No. 02-2615 presented at the Transportation Research Board 81st Annual Meeting, Washington, D.C.

Broek, D. (1982). *Elementary engineering fracture mechanics*, Martinus Nijhoff Publishers, The Hague, The Netherlands.

Brown, E. R. (1992). "Evaluation of SMA used in Michigan." National Center for Asphalt Technology, NCAT Report No.93-3, Auburn, AL.

Brown, S. F., Thom, T. H., and Sanders, P. J. (2001). "A study of grid reinforced asphalt to combat reflection cracking." *J. Assoc. Paving Technologists*, Vol. 70, 543-571.

BRRC, Belgian Road Research Center. (1998). "Design of overlaid cement concrete pavements reinforced with Bitufor® traffic loading." Research report EP5035/3544, Brussels, Belgium.

Button, J. W., and Lytton, R. L. (1987). "Evaluation of fabrics, fibers and grids in overlays." *Proc., 6th International Conference on Structural Design of Asphalt Pavements*, Vol. 1, Ann Arbor, Michigan, 925-934.

Coni, M., and Bianco, P. M. (2000). "Steel reinforcement influence on the dynamic behavior of bituminous pavement." *Proc., 4th International RILEM Conference – Reflective Cracking in Pavements*, E & FN Spon, Ontario, Canada, 3-12.

Erkens, S. M. J. G., Groenendijk, J., Moraal, J., Molenaar, A. A. A., and Jacobs, M. M. J. (1997). "Using Paris' Law to determine fatigue characteristics – A discussion." *Proc., Eight International Conference on Asphalt Pavements*, Seattle, Washington, 1123-1140.

Francken, L., and Vanelstraete, A. (1992). "Interface systems to prevent reflective cracking." *Proc., 7th International Conference on Asphalt Pavements*, International Society for Asphalt Pavements, Nottingham, UK, 45-60.

Halim, A. O., Haas, R., and Phang, W. A. (1983). "Geogrid reinforcement of asphalt pavements and verification of elastic theory." *Transportation Research Record 949*, Transportation Research Board, Washington, D.C., 55-65.

Jacobs, M. M. J., De Bondt, A. H., Molenaar, A. A. A., and Hopman, P. C. (1992). "Cracking in asphalt concrete pavements." *Proc., 7th International Conference on Structural Design of Asphalt Pavements*, Vol. 1, Nottingham University, U.K., 89-105.

Kanninen, M. F., and Popelar, C. H. (1985). *Advanced fracture mechanics,* Oxford University Press, Inc., New York, NY.

Kennepohl, G., Kamel, N., Walls, J., and Hass, R. C. (1985). "Geogrid reinforcement of flexible pavements design basis and field trials." *Proc., Annual Meeting of the Association of Asphalt Paving Technologists*, Vol. 54, San Antonio, TX, 45-75.

Makela, H., Lehtonen, J. and Kallio, V. (1999). "Finnish experiences in preventing frost damages of roads by using steel meshes." *Geotechnical Engineering for Transportation Infrastructure*, Rotterdam, Finland, 1335-1340.

Paris, P. C. and Erdogan, F. A. (1963). "Critical analysis of crack propagation laws." *Transactions of the ASME, Journal of Basic Engineering*, Series D, No. 3, 528-533.

Rice, J. R. (1968). "Mathematical analysis in the mechanics of fracture." *Fracture-An Advanced Treatise*, Vol. II, Academic, New York, 191-308.

Rigo, J. M. (1993). "General introduction, main conclusions of 1989 conference on reflective cracking in pavements, and future prospects." *Proc., 2nd International RILEM Conference – Reflective Cracking in Pavements*, E & FN Spon, Liege, Belgium, 3-20.

Uzan, J. (1997). "Evaluation of fatigue cracking." *Transportation Research Record 1570*, Transportation Research Board, Washington, D.C., 89-95.

Vanelstraete, A., and Francken, L. (2000). "On site behavior of interface systems." *Proc., 4th International RILEM Conference – Reflective Cracking in Pavements*, E & FN Spon, Ontario, Canada, 517-526.